



Patient-specific high tibial osteotomy for varus malalignment: 3D-printed plating technique and review of the literature

Stacy H. Jeong¹ · Linsen T. Samuel¹ · Alexander J. Acuña¹ · Atul F. Kamath¹

Received: 13 January 2021 / Accepted: 28 April 2021 / Published online: 20 June 2021
© The Author(s), under exclusive licence to Springer-Verlag France SAS, part of Springer Nature 2021

Abstract

Purpose We report our experience with a 3D patient-specific instrument (PSI) in an opening-wedge tibial osteotomy for the correction of varus malalignment in a patient with prior anterior cruciate ligament reconstruction. Previous studies have not reported the use of 3D PSI in patients with prior knee surgeries.

Methods A pre-operative CT was used to create a 3D model of the lower extremity using *Bodycad Imager*. The pre-operative medial proximal tibial angle (MPTA), lateral distal femoral angle, hip-knee-ankle (HKA), and tibial slope were calculated. The *Bodycad Osteotomy* software package was used to create a simulated osteotomy and correction. The resulting 3D patient-specific surgical guide and plate were used to conduct the high tibial osteotomy. Radiographic measurements and range of motion were evaluated at 6-week follow-up.

Results The arthroscopy and open portions of the procedure were performed in 65 min, with only three fluoroscopy shots taken intraoperatively. At 6-week follow-up, the patient had 125° of flexion and minimal pain. The angular correction of the bone was achieved within 1.9° (planned MPTA 91.9° vs. actual 90°); the HKA angle was achieved with an error of 0.7° (planned 2.4° vs. actual 1.7°); and there was no change in the posterior tibial slope (planned 13.5° vs 13.8° actual).

Conclusion Three-dimensional PSI can be successfully used for the accurate and efficient correction of varus malalignment while accommodating pre-existing hardware, with good short-term clinical outcomes.

Keywords High tibial osteotomy (HTO) · Opening-wedge osteotomy · 3D printing · Patient-specific

Introduction

High tibial osteotomies (HTO) are indicated for younger patients with isolated medial osteoarthritis of the tibiofemoral compartment [1], with good range of motion and no ligamentous instability. The goal of the osteotomy is to reduce the load on the affected compartment and correct the lower limb malalignment [2]. While both HTO and arthroplasty can slow the progression of osteoarthritis, HTO offer the advantages of preserving bone and having no permanent activity restrictions [2, 3] in the young and active patient.

Correction of the coronal angle is essential in HTO. Overcorrection can lead to patellar subluxation, patella baja, and

lateral compartment osteoarthritis [3]. Under-correction can lead to progression of medial compartment osteoarthritis. While overcorrection into the lateral compartment is generally agreed upon for the weight-bearing axis, there is no consensus on the exact degree of overcorrection [1, 4, 5]. In addition, multiplanar deformities of the tibia require consideration of both the coronal and sagittal planes and thus require monitoring of the tibial slope [6, 7].

Several challenges exist for the pre-operative planning and intraoperative execution of HTO. Pre-operative planning using weight-bearing radiographs is used to calculate the corrective coronal-plane angle [4]. However, variable positioning during radiography may alter limb rotation and thus lead to disparities between planned and actual goal angles [5]. Radiographs also only provide a two-dimensional analysis and cannot be reliably replicated intraoperatively for the monitoring of dual-plane corrections, including coronal balance and sagittal tibial posterior slope [4]. Intraoperative verification using a radiopaque bar or instrument has also been used but carries the disadvantages of increasing

✉ Atul F. Kamath
kamatha@ccf.org

¹ Department of Orthopaedic Surgery, Center for Hip Preservation, Orthopaedic and Rheumatologic Institute, Cleveland Clinic Foundation, 9500 Euclid Avenue, Cleveland, OH 44195, USA

radiation exposure and taking measurements in non-weight-bearing status. Recently, computer navigation systems have provided improvements in achieving coronal alignment while monitoring tibial slope [3]. However, disadvantages such as a higher complication rate, longer operating time, increased equipment, and higher costs must be considered [6].

The use of three-dimensional (3D) patient-specific instruments (PSI) in opening-wedge HTO (OWHTO) has been proposed as an alternative that addresses multiplanar deformities while overcoming the challenges of pre-operative planning and intraoperative execution. Previous studies have reported accurate correction of coronal and sagittal angles [8–12]. Additional advantages reported include reduced operating time, radiation exposure, infection rate, and blood loss [6, 13]. Three-dimensional may offer other benefits in severe deformities, or those with prior surgical hardware and iatrogenic deformity.

We report our experience with 3D PSI in an opening-wedge tibial osteotomy for the correction of varus malalignment in a patient with prior anterior cruciate ligament (ACL) reconstruction. Previous studies have not reported the use of 3D PSI in patients with prior knee surgeries. We hypothesized that the use of 3D PSI in this case would increase reproducibility and accuracy to pre-operative plan, reduce risk of iatrogenic fracture with the existing ACL tunnel, and address the multiplanar deformity in an efficient surgical method.

Case report

A 38-year-old male presented with symptomatic right knee pain, with medial compartment arthrosis and varus malalignment of the knee. He previously had undergone an ACL reconstruction but no bony correction of the limb malalignment. He had failed non-surgical measures including physical therapy, unloader bracing, and injection therapy. He was indicated for OWHTO of the right knee.

Computer-assisted pre-operative planning

A computed tomography (CT) scan of the patient's right knee was performed with a slice thickness of 1 mm. Digital Imaging and Communications in Medicine (DICOM) data were extracted by proprietary software (*Bodycad Imager*, Bodycad, Quebec, Canada), and a 3D model of the femur, tibia, and fibula was created. The pre-operative planning was performed using the *Bodycad Osteotomy* software package (Bodycad, Quebec, Canada). True anteroposterior (AP) and lateral views were created by overlapping the

Fig. 1 Pre-operative coronal long-standing AP radiograph with overlapping 3D bone modeling

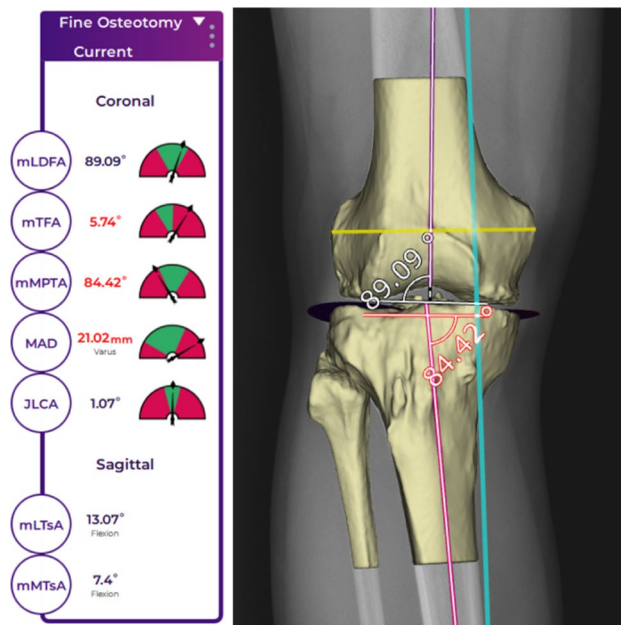
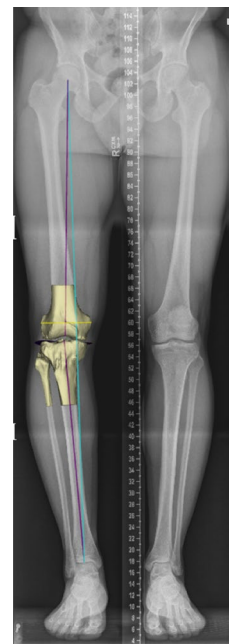


Fig. 2 Pre-operative angular measurements in the coronal (3D model presented) and sagittal planes

bone model on the patient's long-standing AP radiograph (Fig. 1). Different landmarks were positioned over the 3D bone model by the software; pre-operative measurements and angles such as MPTA (medial proximal tibial angle), LDFA (lateral distal femoral angle), HKA (hip-knee-ankle), and tibial slope were calculated (Fig. 2). The

patient had a normal JLCA (joint line convergence angle) value of 1.07°, a tibiofemoral varus alignment of 5.74°, a MPTA of 84.42°, and medial and lateral tibial slope of 7.40° and 13.47°, respectively.

Following the final checks by the senior author and surgeon, the simulated osteotomy and correction were made using the *Bodycad Osteotomy* software. The WBL (weight-bearing line) correction to 55% of the tibial plateau width was chosen. An opening of 10.21 mm was calculated by the software to obtain this particular correction. The resulting patient’s lower limb alignment was calculated to be a tibiofemoral valgus alignment of 1.69° and a MPTA of 91.86°, with no change of the tibial slope (Figs. 3, 4). The hinge axis was planned to be at an ideal position of 15 mm from the lateral plateau and 10 mm from the lateral cortex. A biplane cut was proposed due to the tibial tuberosity that was in the way of the osteotomy cutting plane. The cut was positioned just below the ACL screw (Fig. 5). Approval of the pre-operative planning was done prior to manufacturing the patient-specific surgical guide and plate (Figs. 6, 7 and 8).

Surgical technique

The patient was placed under general anesthesia. An arthroscopy of the knee was made prior to the osteotomy; a partial medial meniscectomy and chondroplasty of the medial compartment were performed. The ACL graft was

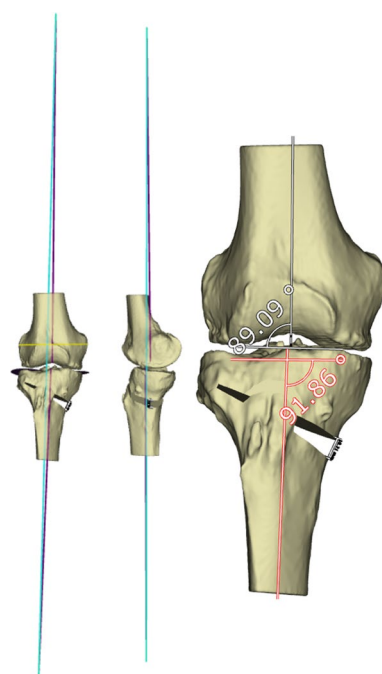


Fig. 4 Virtual correction for a planned 10.21 mm medial opening wedge osteotomy, resulting in a weight-bearing axis line 55% of the tibial width when measured from the medial tibial plateau

intact. Next, attention was turned to the proximal tibia for exposure of the OWHTO site. A 7-cm longitudinal skin incision at the anteromedial aspect of the proximal tibia, between the patellar tendon and the medial collateral ligament, was made in standard fashion. Prior to placing the cutting guide, the 3D-printed sterile bone model was used to confirm the position and contact region of the surgical guide over the bone. Temporary fixation screws were used

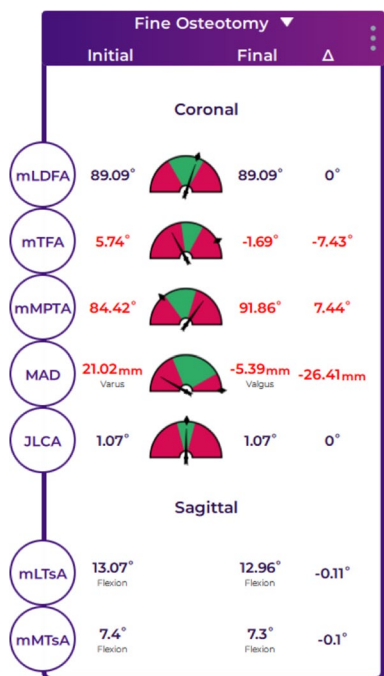
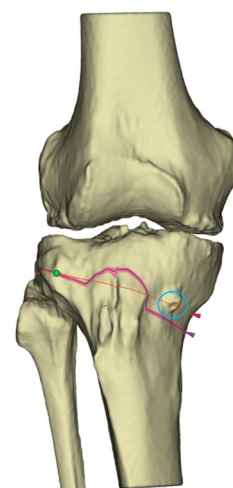


Fig. 3 Virtual osteotomy pre-operative plan angular parameters

Fig. 5 Virtual position of the biplanar cut (red line) just below the ACL reconstruction screw (circled in blue). The hinge axis point has been defining at the ideal position (green dot), which lies 15 mm below the joint line and 10 mm from the lateral tibial cortex in this patient



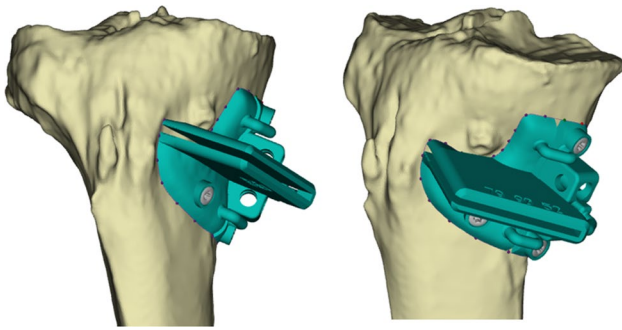


Fig. 6 Design of the patient-specific surgical guide to perform the osteotomy and introduce the plate and screws about the existing ACL screw and tunnel

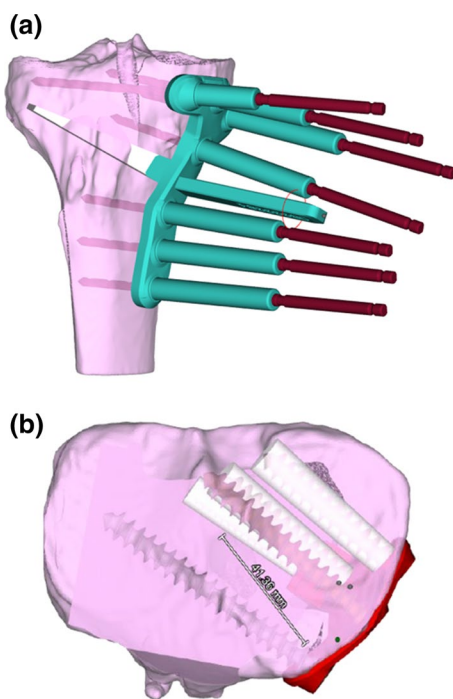


Fig. 7 Pre-drilling guide (teal) and associated calibrated drill bit (red) (a). The existing ACL tunnel and screw are visualized, and custom trajectories are presented in the transverse plane (b)

to fasten the guide in place (Fig. 9). Two drilling towers were locked into the surgical guide (Fig. 10). Using a pre-calibrated drill (with depth control), multiple holes cortical perforations were made at the osteotomy location. The drilling towers were then removed, so that the surgeon had access to a slot to insert a calibrated osteotome to finish the cut. The anterior part of the surgical guide was then clipped off and removed, leaving only the posterior part over the patient's bone. The biplane vertical cut behind the patellar

tendon was finished using an osteotome. A fluoroscopy shot was made to confirm the completion of the cut. The calibrated bone spreader was inserted into the anchors (posterior section of the guide which was left in place) (Fig. 11). Using the bone spreader, the osteotomy was slowly distracted with precise control. The osteotomy site was spread until it reached the planned correction, then slightly overcorrected to 11 mm to allow for placement of void filler and the plate (Fig. 12). Since the design of the plate was overlapping with the anchor boxes, a lamina spreader and a 3D-printed validator block were inserted into the osteotomy to be able to remove the bone spreader and the anchors boxes (Fig. 13). The pre-drill guide was inserted over the bone and used to pre-drill the plate's screw hole using a depth-controlled drill. The plate was then inserted on the bone, and temporary fixation pins were used to maintain alignment of the plate with the pre-drilled holes. Only the four proximal screw holes and the first distal screw holes were pre-drilled using this technique. The remaining screw holes were drilled through a drill tower that locked into the plate. A patient-specific sterile planning card (anodized aluminum) was provided with the plate and screws to confirm with the surgeon which screws (type and length) were to be placed in each of the specific screw holes (Fig. 14). The screws were then inserted in the plate (Fig. 15) and seated flush (Fig. 16). A 7 mm synthetic beta-tricalcium phosphate graft (*OSFerion Osteotomy Wedge*, Arthrex, Naples, the USA) was used to fill the gap. Two fluoroscopy shots (frontal and lateral views) were taken to confirm the implant placement and screw positions (Fig. 17).

The arthroscopy and open portions of the procedure were performed in 65 min. The entire osteotomy was performed in full extension due to the help of the patient-specific surgical guide to minimize dissection, and the calibrated drills to avoid over-penetration of the posterior soft tissues. Three still shots of intraoperative fluoroscopy were made during the procedure: One after the osteotomy was performed and two after the final implant had been affixed to the patient.

At 6-week follow-up, the patient's range of motion was full extension to 125° of flexion with a well-healed incision and minimal pain. The patient was using acetaminophen as needed for pain. He was continuing with a physical therapy protocol. Radiographs taken at this 6-week visit demonstrated a satisfactory stage of healing, with a precise correction in the coronal and sagittal planes (Fig. 18). The angular correction of the bone was achieved within 1.9° (planned MPTA 91.9° vs. actual 90°); the HKA angle was achieved with an error of 0.7° (planned 2.4° vs. actual 1.7°); and there was no change in the posterior tibial slope (planned 13.5° vs 13.8° actual) (Fig. 19).

Fig. 8 Design of the patient-specific plate, including an intra-cortical plate wedge to sit precisely inside the 10.2 mm osteotomy gap

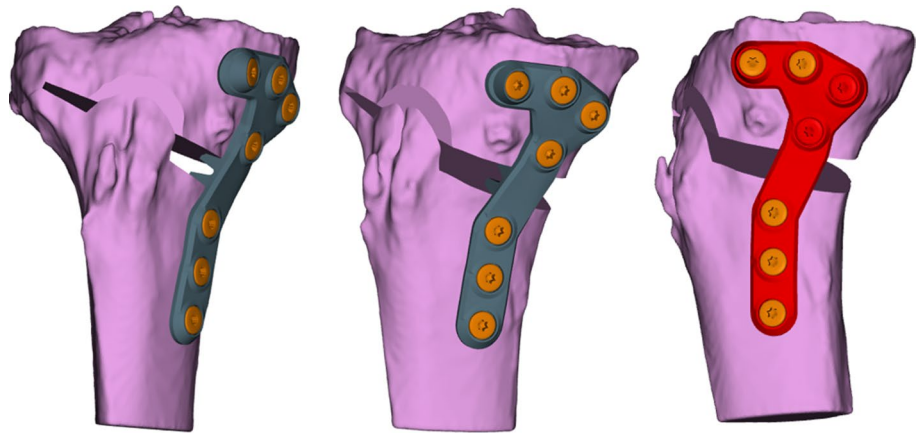


Fig. 9 Placement of the patient-specific surgical guide intraoperatively

Discussion

This study showed successful use of a 3D PSI-guided HTO to correct varus malalignment in a patient with prior ACL reconstruction. Previous studies with 3D PSI have not included patients with pre-existing hardware. High tibial osteotomy requires extensive pre-operative planning due to the high degree of precision required for multiplanar correction. In our study, custom planning was used to create a patient-specific plan, osteotomy guides, and patient-specific plate to perform an exacting correction while accommodating the prior ACL tunnel and hardware.

The correction of lower limb malalignment with HTO poses several challenges and risks. Dean et al. reported

complication rates from HTO ranging from 0 to 47% [14]. Adverse events include deep vein thrombosis, nerve injury, and intra-operative fractures, including lateral hinge fracture, cortical fracture, and tibial plateau fracture [15, 16]. Under-correction of varus malalignment can lead to progression of medial compartment osteoarthritis and patient dissatisfaction [4, 17]. The current literature agrees on overcorrection into valgus alignment [1, 4, 5]. However, the optimal angle has not been determined, and the recommendations vary from 3° to at least 8° [1, 9, 10]. Moreover, the ideal correction is patient-specific and multiplanar. Abnormal joint line obliquity from overcorrection into valgus also may have negative clinical outcomes. Akamatsu et al. compared patients with overcorrected MPTA (>95°) with those with normal MPTA after HTO. They found no significant difference in medial cartilage preservation and lateral cartilage degeneration between the cohorts, but reported lower postoperative Knee Injury and Osteoarthritis Outcome Score (KOOS) and American Knee Society knee and function scores (AKS) in the increased MPTA cohort [11]. Goshima et al. found no significant difference in cartilage degeneration, and no significant differences in Japanese Orthopedic Association score (JOA), 12-item Oxford Knee Score (OKS), or KOOS scores after a mean follow-up of 6.1 years [12]. However, these studies assessed the cartilage at a mean of 12 months and 18.5 months, respectively. An earlier study by Hernigou et al. reported that all 5 knees with 6 degree postoperative valgus showed degenerative changes in the lateral component in a 10- to 13-year follow-up study [17]. In addition to lateral osteoarthritis, overcorrection into valgus can lead to patellar subluxation, patella baja, and medial joint opening [4, 17, 18].

In addition to malalignment in the coronal plane, tibial deformities often also occur in the sagittal plane [17]. Medial opening-wedge HTOs can also unintentionally increase tibial posterior slope [19]. The increase in tibial posterior slope is attributed to the perpendicular orientation of the lateral

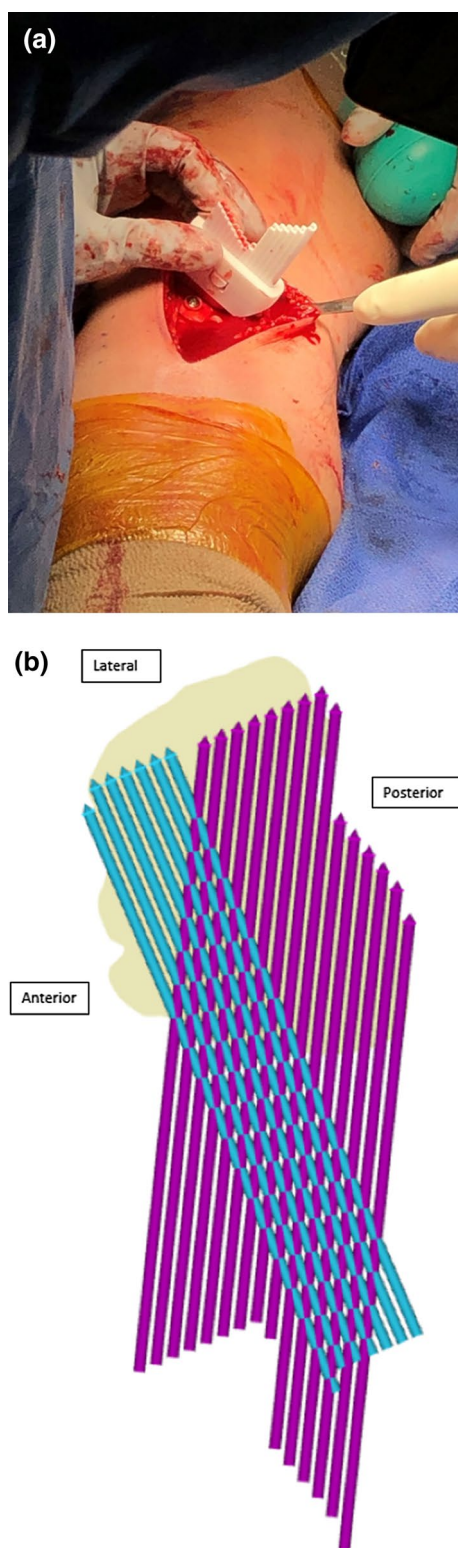


Fig. 10 Insertion of the drilling tower intraoperatively (a) to perform the osteotomy using a depth-controlled drilling technique. The depths are determined as part of the pre-operative plan as visualized in the transverse plane (b)

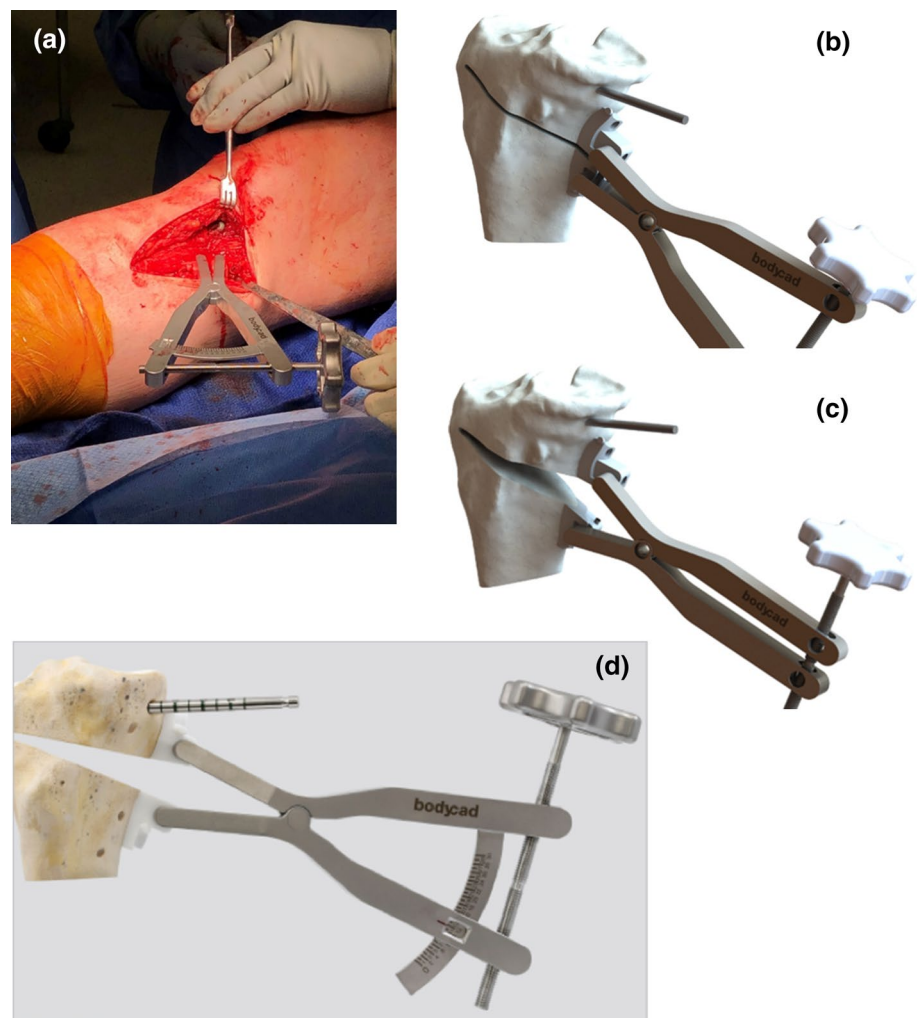
tibial cortex, incomplete osteotomy of the posterolateral cortex, and incomplete release of posterior soft tissue [7, 8, 20]. This can lead to anterior tibial translation, subluxation of the tibia, and increased load on the ACL [6, 7, 20]. Marti et al. reported that tibial posterior slope greater than 10° can theoretically increase ACL tensile load by threefold [19].

Current conventional methods for HTO planning have variable success in the execution of the planned coronal angle and poor maintenance of appropriate tibial posterior slope. Pre-operative planning using radiographs can lead to deviation in planned and executed angles due to variable limb rotation during positioning [13, 14]. These also cannot be used intraoperatively, making it challenging to monitor changes in tibial posterior slope. Studies using these methods report increases in tibial posterior slope ranging from 2.2° to 4.2° [17, 21, 22]. Tibial posterior slope must especially be monitored for HTO with concomitant ACL reconstruction to prevent stretch of the ACL graft [19]. Intra-operative use of fluoroscopy for measurement of lower limb alignment is commonly used. In this method, a radiopaque line is created with either a fixed rod or a Bovie cord extended from the center of the femoral head to the center of the ankle joint [23]. This allows for intraoperative monitoring but can lead to unsatisfactory correction due to the patient's non-weight-bearing status during measurement [4, 24], along with any fluoroscopic distortion.

Several studies have reported low accuracy and low reproducibility of these conventional methods of planning. Van den Bempt et al. conducted a review of 15 studies comparing 14 cohorts that used conventional method HTOs, including radiopaque instrument measurements, to 9 cohorts that used computer-navigated HTOs. This study found that 8 of the 14 conventional cohorts reported a success rate below 75% in achieving postoperative correction within an accepted range of accuracy [18]. The success rate varied between 23 and 92% in these conventional cohorts. Bae et al. found similar findings, reporting an 86% reproducibility in the navigated cohort compared to 50% reproducibility in the conventional cohort with respect to achieving a mechanical axis of 3° [20]. While Yan et al. and Wu et al. also reported greater accuracy of mechanical axis alignment using navigated HTOs, both these studies found no significant differences in clinical outcomes between the conventional and navigated cohorts [21, 22].

Several studies have shown accurate multiplanar correction using 3D PSI for lower limb osteotomies. Victor and Premanathan conducted the first pilot study using 3D planning for tibial and femoral osteotomies [25]. They reported a mean difference in planned and postoperative wedge angle of 0° (range, -1 to 1 ; SD 0.72) in the coronal plane and 0.3° (range, -0.9 to 3 ; SD 1.14) in the sagittal plane using

Fig. 11 The calibrated bone spreader seated within the anchor boxes of the 3D-printed surgical guide prior to opening of the osteotomy site (a). The spreader allows for precise degree corrections (b–d) in a controlled fashion



radiographs for analysis. However, this study did not assess tibial posterior slope. Yang et al. used radiographic analysis for pre-operative and postoperative measurements and reported an error of 4.9% for weight-bearing line (WBL) and 4.1% for tibial slope, but did not report errors in the coronal angle [6]. Donnez et al. conducted a CT-scan controlled study in cadavers; they reported a mean difference of 0.2° (range, -0.3 to 0.5 ; SD 0.3) in the coronal plane and difference of -0.1° (range, -0.7 to 0.8 ; SD 0.5) in the sagittal plane [26]. Munier et al. used 2D and 3D analysis with a CT-based postoperative reconstruction of the tibia. They reported a mean difference of 0.98° (range, 0.92 to 0.99) for hip-knee-ankle angle (HKA) and 0.96° (range, 0.79 to 0.99) for tibial slope using radiographic analysis, with comparable measurements in the 3D analysis [27].

Two studies have compared 3D PSI to conventional planning methods in high tibial osteotomy. Pérez-Mañanes et al. reported a mean difference between planned and postoperative wedge angle of 0.5° (range, 0 to 1.2) for the 3D technique and a mean difference of 1.1° (range, 0 to 2.8) in the conventional technique. However, there was no significant difference between the two techniques for both the difference in wedge angle and final valgus angle [13]. However, the method used for conventional planning was not specified. Kim et al. compared the use of 3D PSI with pre-operative planning with digital radiography. They found comparable results between 3D and radiography groups for postoperative weight-bearing line, mechanical tibiofemoral angle, and posterior tibial slope angle, but reported a significantly higher number of patients with values within acceptable range in the 3D group [28]. No studies have compared 3D PSI to



Fig. 12 Use of the bone spreader to accurately open the osteotomy at the pre-operative opening (10.2 mm). The ACL screw is visualized in this image. The 3D-printed bone model with ideal correction has been used for reference

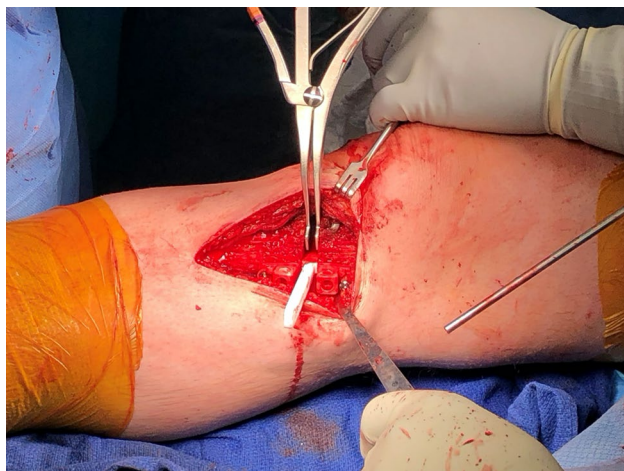


Fig. 13 A lamina spreader and the validator block were used to maintain the osteotomy opened while removing the bone spreader and the anchor block

computer-navigated systems. However, studies comparing conventional methods to navigated systems reported longer operating times and higher rates of infection with navigated systems [6, 22, 29]. Complications from the five 3D PSI studies include one spontaneously resolving hematoma reported by Munier et al., and one patient who developed a

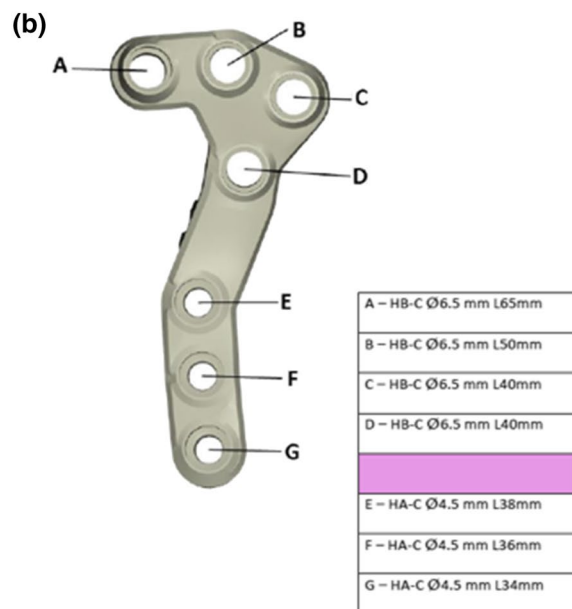
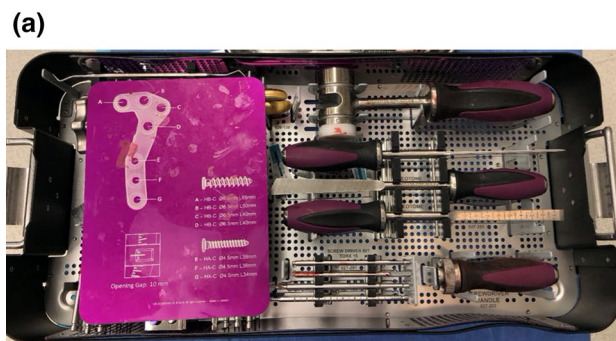


Fig. 14 Anodized aluminum card (patient-specific planning) informs the surgeon which screws are to be used in the respective plate holes, along with the single instrument tray for the entire procedure (a). The screw lengths are also included in the formal pre-operative plan (b)



Fig. 15 Temporary fixation pegs are placed in the pre-drilled screw holes to stabilize the plate while inserting the definitive screws

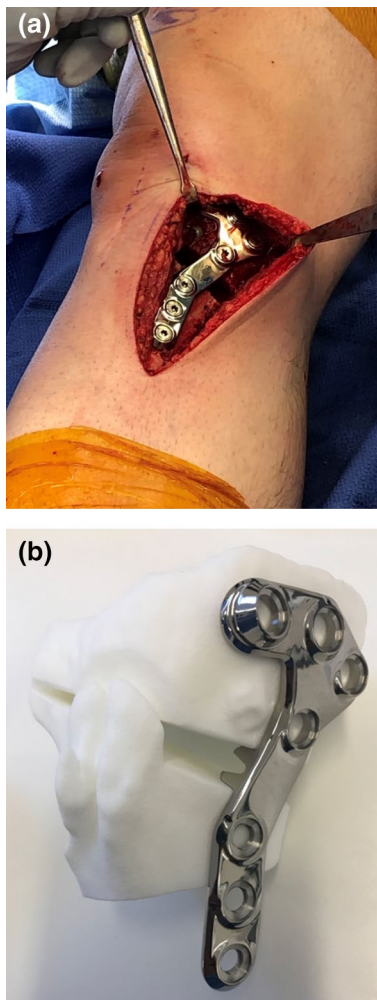
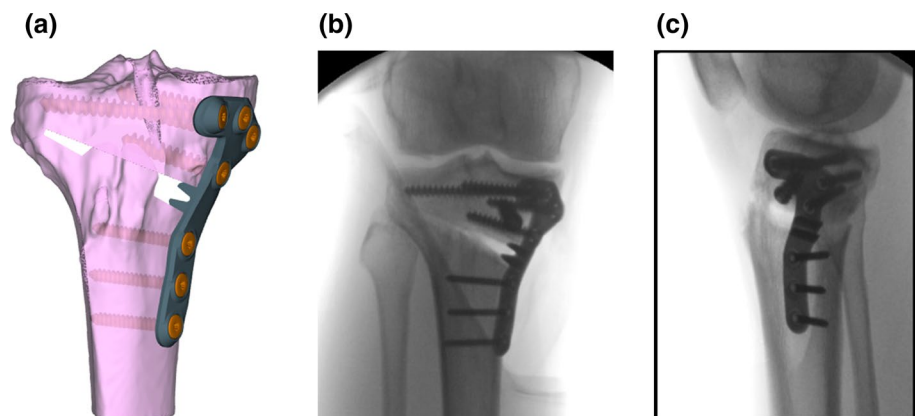


Fig. 16 Intraoperative view of the final implant (a), along with the pre-operative bone model (b)

delayed union treated with iliac crest autografting by Victor et al. [25, 27].

Our procedure demonstrated a high degree of accuracy between planned procedure and intra-operative execution. This supports previous literature on the precision and accuracy of bi-planar correction using 3D PSI, with no intraoperative complication in our procedure. Other benefits include the ability to plan screw and plate placement, as well as plate configuration to match the bone, prior hardware, and existing deformities. Only three intraoperative fluoroscopic images were taken compared to an average of 55 images reported with conventional methods [13], thus reducing radiation exposure to the patient and surgeon. Other studies reported similar reductions in intraoperative fluoroscopy that may mitigate the initial radiation from pre-operative CT scanning [6, 13]. Drilling reduced possible thermal necrosis and bone loss which occurs with a large-kerf saw. The calibrated opening bone spread also allowed for precise opening and maintenance of correction and validation of the wedge opening. The calibrated osteotomy and drilling technique reduced chance of neurovascular injury and risk of iatrogenic fracture with the patient's existing hardware and ACL tunnel. Pre-drilling of plate screws through the guide also reduced issues with screw purchase and placement, as well as low-profile plate and instrumentation that aided with minimizing soft tissue irritation. Overall, the use of 3D PSI increased intraoperative efficiency with a single instrument tray, reduced fluoroscopy time, and custom guides and plate, while achieving accurate correction of limb malalignment with no witnessed complications. A future study should assess long-term outcomes, including patient-reported outcomes and clinical follow-up, of this patient-specific, precise osteotomy technique.

Fig. 17 Comparison of the virtual implant and screw orientation (a) with the final implant placement in coronal (b) and sagittal (c) fluoroscopic projections



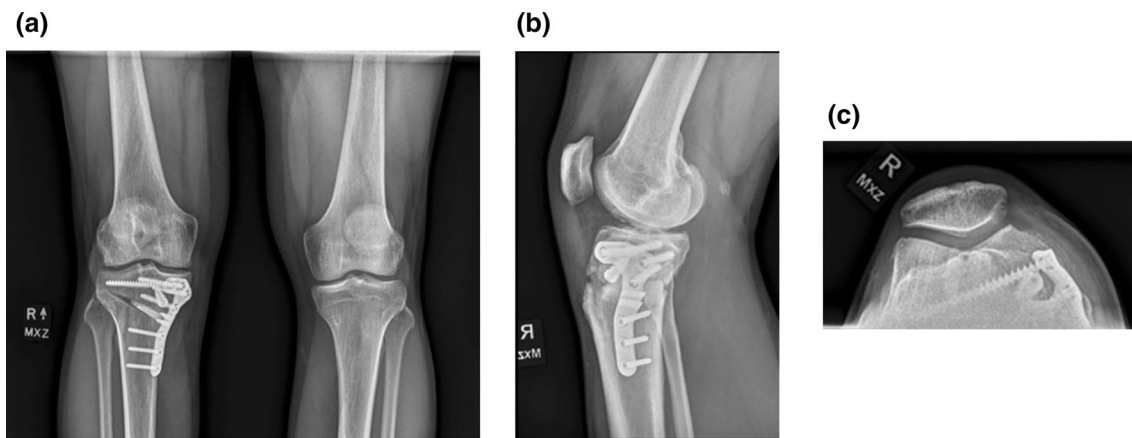


Fig. 18 Anteroposterior weight-bearing (a), lateral (b), Merchant (c), and full-length standing (d) radiographs taken at 6 weeks post-surgery

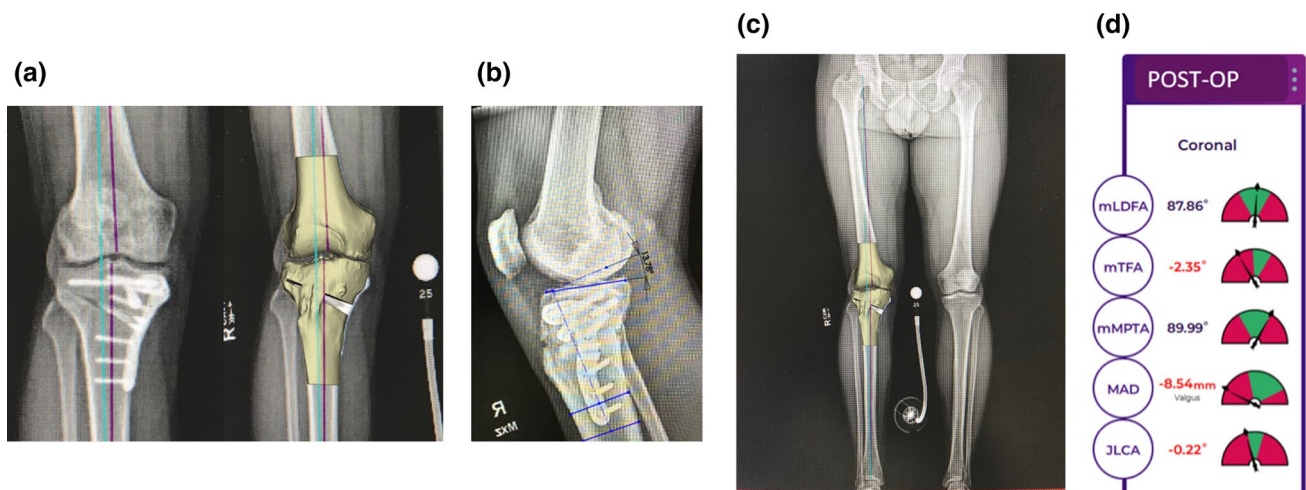


Fig. 19 Anteroposterior weight-bearing (a), lateral (b), and full-length standing (c) postoperative radiographs taken at 6 weeks with accuracy analysis superimposed. The formal angular measurements are visualized in the software platform (d)

Funding No funding was received for this study.

Declarations

Ethical declaration We certify that our analysis complies with the ethical standards of our institution as well as laws related to research conducted in the USA.

Conflict of interest A.F.K. reports the following disclosures: research support (Signature Orthopaedics), paid presenter or speaker (DePuy Synthes and Zimmer Biomet), paid consultant (DePuy Synthes and Zimmer Biomet), stock or stock options (Zimmer Biomet, Johnson & Johnson, and Procter & Gamble), IP royalties (Innomed), and board or committee member (AAOS, AAHKS, and Anterior Hip Foundation). L.T.S., A.J.A., J.M.K., and A.E. have nothing to disclose.

References

- Rossi R, Bonasia DE, Amendola A (2011) The role of high tibial osteotomy in the varus knee. *J Am Acad Orthop Surg* 19(10):590–599. <https://doi.org/10.5435/00124635-201110000-00003>
- DeBarge R, Trouillet F, Demey G, Magnussen RA (2014) High tibial osteotomy. *Surg Knee* 24:149–161
- Akamatsu Y, Mitsugi N, Mochida Y, Taki N, Kobayashi H, Takeuchi R et al (2012) Navigated opening wedge high tibial osteotomy improves intraoperative correction angle compared with conventional method. *Knee Surg Sport Traumatol Arthrosc* 20:586–593
- Kwun J-D, Kim H-J, Park J, Park I-H, Kyung H-S (2017) Open wedge high tibial osteotomy using three-dimensional printed models: experimental analysis using porcine bone. *Knee* 24:16–22

5. Kawakami H, Sugano N, Yonenobu K, Yoshikawa H, Ochi T, Hattori A et al (2004) Effects of rotation on measurement of lower limb alignment for knee osteotomy. *J Orthop Res* 22:1248–1253
6. Yang JCS, Chen CF, Luo CA, Chang MC, Lee OK, Huang Y et al (2018) Clinical experience using a 3D-printed patient-specific instrument for medial opening wedge high tibial osteotomy. *Biomed Res Int* 2018
7. Jones GG, Jaere M, Clarke S, Cobb J (2018) 3D printing and high tibial osteotomy. *EFORT Open Rev Br Ed Soc Bone Jt Surg* 3:254–259
8. Martin R, Birmingham TB, Willits K, Litchfield R, Lebel M-E, Giffin JR (2014) Adverse event rates and classifications in medial opening wedge high tibial osteotomy. *Am J Sports Med* 42:1118–1126
9. Coventry MB (1965) Osteotomy of the upper portion of the tibia for degenerative arthritis of the knee: a preliminary report. *J Bone Joint Surg Am* 47:984–90
10. Ivarsson I, Myrnerets R, Gillquist J (1990) High tibial osteotomy for medial osteoarthritis of the knee. A 5 to 7 and an 11 to 13 year follow-up. *J Bone Jt Surg Ser B* 72:238–244
11. Akamatsu Y, Kumagai K, Kobayashi H, Tsuji M, Saito T (2018) Effect of Increased coronal inclination of the tibial plateau after opening-wedge high tibial osteotomy. *Arthrosc J Arthrosc Relat Surg* 34:2158–2169
12. Goshima K, Sawaguchi T, Shigemoto K, Iwai S, Fujita K, Yamamuro Y (2019) Comparison of clinical and radiologic outcomes between normal and overcorrected medial proximal tibial angle groups after open-wedge high tibial osteotomy. *Arthroscopy* 35:2898–2908
13. Pérez-Mañanes R, Burró JA, Manaute JR, Rodríguez FC, Martín JV (2016) 3D Surgical printing cutting guides for open-wedge high tibial osteotomy: do it yourself. *J Knee Surg* 29:690–695
14. Dean CS, Liechti DJ, Chahla J, Moatshe G, LaPrade RF (2016) Clinical outcomes of high tibial osteotomy for knee instability: a systematic review. *Orthop J Sport Med* 4:2325967116633419
15. Noyes FR, Goebel SX, West J (2005) Opening wedge tibial osteotomy: the 3-triangle method to correct axial alignment and tibial slope. *Am J Sports Med* 33:378–387
16. El-Azab H, Halawa A, Anetzberger H, Imhoff AB, Hinterwimmer S (2008) The effect of closed- and open-wedge high tibial osteotomy on tibial slope: a retrospective radiological review of 120 cases. *J Bone Jt Surg Ser B* 90:1193–1197
17. Hernigou P (2002) Open wedge tibial osteotomy: combined coronal and sagittal correction. *Knee* 9:15–20
18. Van den Bempt M, Van Genechten W, Claes T, Claes S (2016) How accurately does high tibial osteotomy correct the mechanical axis of an arthritic varus knee? A systematic review. *Knee* 23:925–935
19. Marti CB, Gautier E, Wachtl SW, Jakob RP (2004) Accuracy of frontal and sagittal plane correction in open-wedge high tibial osteotomy. *Arthroscopy* 20:366–372
20. Bae DK, Song SJ, Yoon KH (2009) Closed-wedge high tibial osteotomy using computer-assisted surgery compared to the conventional technique. *J Bone Jt Surg Ser B* 91:1164–1171
21. Yan J, Musahl V, Kay J, Khan M, Simunovic N, Ayeni OR (2016) Outcome reporting following navigated high tibial osteotomy of the knee: a systematic review. *Knee Surg Sport Traumatol Arthrosc* 24:3529–3555
22. Wu ZP, Zhang P, Bai J, Liang Y, Chen PT, He JS et al (2018) Comparison of navigated and conventional high tibial osteotomy for the treatment of osteoarthritic knees with varus deformity: a meta-analysis. *Int J Surg* 55:211–219
23. Jang K-M, Lee J-H, Cho IY, Park B-K, Han S-B (2017) Intraoperative fluoroscopic assessment of limb alignment is a reliable predictor for postoperative limb alignment in biplanar medial opening-wedge high tibial osteotomy. *J Arthroplasty* 32:756–760
24. Yoon S-D, Zhang G, Kim H-J, Lee B-J, Kyung H-S (2016) Comparison of cable method and miniaci method using picture archiving and communication system in preoperative planning for open wedge high tibial osteotomy. *Knee Surg Relat Res* 28:283–288
25. Victor J, Premanathan A (2013) Virtual 3D planning and patient specific surgical guides for osteotomies around the knee: a feasibility and proof-of-concept study. *Bone Jt J* 95-B:153–158
26. Donnez M, Ollivier M, Munier M, Berton P, Podgorski JP, Chabrand P et al (2018) Are three-dimensional patient-specific cutting guides for open wedge high tibial osteotomy accurate? An in vitro study. *J Orthop Surg Res* 13:171
27. Munier M, Donnez M, Ollivier M, Flecher X, Chabrand P, Argenson J-N et al (2017) Can three-dimensional patient-specific cutting guides be used to achieve optimal correction for high tibial osteotomy? Pilot study *Orthop Traumatol Surg Res* 103:245–250
28. Kim HJ, Park J, Shin JY, Park IH, Park KH, Kyung HS (2018) More accurate correction can be obtained using a three-dimensional printed model in open-wedge high tibial osteotomy. *Knee Surg Sport Traumatol Arthrosc* 26:3452–3458
29. Hankemeier S, Hufner T, Wang G, Kendoff D, Zeichen J, Zheng G et al (2006) Navigated open-wedge high tibial osteotomy: advantages and disadvantages compared to the conventional technique in a cadaver study. *Knee Surg Sports Traumatol Arthrosc* 14:917–921

Publisher's Note Springer Nature remains neutral with regard to jurisdictional claims in published maps and institutional affiliations.